Published in final edited form as:
Endocrinology. 2003 February ; 144(2): 412–422.

Glucocorticoids Induce Rapid Up-Regulation of Mitogen-Activated Protein Kinase Phosphatase-1 and Dephosphorylation of Extracellular Signal-Regulated Kinase and Impair Proliferation in Human and Mouse Osteoblast Cell Lines

Y. ENGELBRECHT, **H. de WET**, **K. HORSCH**, **C. R. LANGEVELDT**, **F. S. HOUGH**, and **P. A. HULLEY**
Endocrinology and Metabolism Unit, Department of Internal Medicine, University of Stellenbosch, Tygerberg 7505, Cape Town, South Africa

Abstract

A central feature of glucocorticoid (GC)-induced osteoporosis is decreased bone formation, secondary to decreased numbers of functional osteoblasts. We find that ERK activity is essential for serum-induced osteoblast proliferation *in vitro* because inhibition of MAPK/ERK kinase activity by U0126 completely abolished both serum-induced activation of ERK and proliferation of mouse (MBA-15.4) and human (MG-63) osteoblast cell lines. Dexamethasone (Dex) rapidly (<2 h) inhibits the sustained phase of ERK activation, required for nuclear shift and mitogenesis. This inhibition is reversed by cotreatment with the protein synthesis inhibitor, cycloheximide, and by the GC receptor antagonist, RU486, suggesting a classical transcriptional mechanism. Phosphatase activity was up-regulated by Dex treatment, and inhibition of ERK activity by Dex was also reversed by the protein tyrosine phosphatase inhibitor, vanadate. Coupled with the rapidity of Dex action, this indicates immediate-early gene phosphatase involvement, and we therefore used quantitative, real-time PCR to examine expression profiles of the dual-specificity MAPK phosphatases, MKP-1 and MKP-3. MKP-1, but not MKP-3, mRNA expression was 10-fold up-regulated in both mouse and human osteoblast cell lines within 30 min of Dex treatment and remained elevated for 24 h. MKP-1 protein was also markedly up-regulated following 1–8 h of Dex treatment, and this correlated precisely with dephosphorylation of ERK. Cell proliferation was impaired by Dex treatment, and this was reversed by both RU486 and vanadate. Therefore, MKP-1 up-regulation provides a novel and rapid mechanism, whereby GCs inhibit osteoblast proliferation.

Glucocorticoid (GC)-induced osteoporosis is characterized histologically by a decreased bone formation rate, decreased trabecular wall thickness, and depleted osteoblast numbers, all indicators of a deficient osteoblast population (1, 2). This reduction in functional osteoblasts is caused by a combination of factors, which include GC-induced apoptosis, transdifferentiation into adipocytes, and GC-induced impairment in the mitogenic response of preosteoblasts to growth factors (2, 3).

GCs primarily act at the level of gene transcription, where they either activate or repress expression of a variety of genes (4). GCs can also regulate signaling pathways via interactions with membrane receptors and ion-channels in a rapid and transcription-

Address all correspondence and requests for reprints to: Dr. P. A. Hulley, Department of Endocrinology and Metabolism, Faculty of Health Sciences, University of Stellenbosch, P.O. Box 19063, Tygerberg 7505, Cape Town, South Africa. phul@gerga.sun.ac.za. .

Europe PMC Funders Author Manuscripts

independent manner (5), but the effects on osteoblasts appear to be protein synthesis dependent and classical (6). Transcriptional activation occurs when GCs bind to the GC receptor (GR), a cytosolic receptor that, when ligand-occupied, translocates to the nucleus where it binds to and activates the GC response element (GRE) in gene promoters. Repression of transcription by steroids is usually GRE-independent and takes place via protein-protein interactions between the GR and other transcription factors such as nuclear factor-κB and activator protein-1 (4). Inhibition of proliferation by GC could therefore be caused by down-regulation of cell-cycle drivers such as the receptors, adaptors and kinases upstream of ERK and the cell cycle (7-9), or by up-regulation of growth-inhibitory or cell death pathways (2).

Osteoblast proliferation is controlled by multiple pathways, not all of which are understood in detail. Receptor protein tyrosine kinase (RPTK), G protein-coupled, integrin-linked and bone morphogenetic protein-2 signaling mechanisms all involve the ERK pathway to some extent (7-13). RPTKs in particular make use of the Raf-MEK (MAPK/ERK kinase)-ERK MAPK cascade (7, 8). This well-described pathway is strongly dependent on tyrosine phosphorylation steps, starting with RPTK transphosphorylation, recruitment of the Src homology 2 domain containing adaptor proteins shc and grb2, and the activation of Raf. Raf in turn activates MEK, a dual-specificity kinase with exclusive substrate preference for ERK. Phosphorylated ERK moves to the nucleus where it activates the cell cycle machinery (9).

Negative regulation of the ERK pathway takes place through several mechanisms. These include receptor dynamics (14, 15), the inactivation of ras via ras-GTPase-activating protein (GAP) (16), and the negative feedback loop, whereby ERK phosphorylates son-of-sevenless (SOS), the ras guanine nucleotide exchange factor, and dissociates it from grb2 (17). However, the growth factor response pathway is also dephosphorylated by a variety of phosphatases (18-20), and this is the central mechanism under discussion in the present study. Multiple membrane and cytosolic phosphatases act at the receptor and receptor-proximal level; for example, the serine-threonine phosphatase PP2A, which inactivates the ERK cascade in A431 and other cell lines (20), the cytosolic PTP-1B, which negatively regulates insulin signaling, and the Src homology 2 domain-containing protein tyrosine phosphatase (PTP), SHP-1, which inhibits cell growth of several hemopoietic lineages (18, 21). Nuclear ERK is, however, primarily targeted by the dual-specificity phosphatases, which have exclusive substrate preference for the ERK, c-*jun* NH_2-terminal kinase (JNK), and p38 MAPKs (19, 22). This sub-group of PTPs are mostly immediate-early gene products (23, 24), with rapid transcriptional induction following MAPK family activation, short half-lives, and rapid destruction by the 26S proteasome (25). Recently, the dual-specificity MAPK phosphatase (MKP-1) has been reported to be up-regulated by dexamethasone (Dex) in mast cells, with concurrent inactivation of ERK and decreased mast cell proliferation (26). This up-regulation is both GR and protein synthesis dependent and makes use of functional GREs in the promoter region of the MKP-1 gene (26, 27).

We have previously shown that treatment with Dex for 48 h causes up to 70% growth inhibition of the MBA-15.4 preosteoblast cell line, and that this is associated with impaired ERK activity in response to mitogens (3). Both impairment of ERK activation and cell proliferation by Dex are prevented by cotreatment with the PTP inhibitor, sodium orthovanadate (3), implicating PTPs in these processes. Vanadium has been reported to stimulate proliferation of chick (28), rat (29, 30), and human (31) primary osteoblast cultures, and to increase alkaline phosphatase levels and collagen synthesis (31). In addition, we have found that supplementation with sodium orthovanadate reverses the negative effects of high-dose GCs on bone formation and largely prevents the development of steroid osteoporosis in the *in vivo* rat model (32). In this report, we have investigated whether Dex

Europe PMC Funders Author Manuscripts

inhibits osteoblastic growth by transcriptional regulation, and in particular the role played by protein tyrosine phosphatases as inhibitors of ERK activity. We demonstrate that GCs rapidly up-regulate the immediate-early gene phosphatase, MKP-1, in both mouse and human osteoblast cell lines by a classical transcriptional mechanism, with associated excessive dephosphorylation of ERK.

Materials and Methods

Materials

Enhanced chemiluminescence detection reagents, Rainbow molecular weight markers, and paranitrophenylphosphate (pNPP) were purchased from Amersham International (Buckinghamshire, UK). Fetal calf serum was from Delta Bioproducts (Republic of South Africa). RU486 and progesterone were kind gifts from Prof. Janet Hapgood (Department of Biochemistry, University of Stellenbosch, Tygerberg, Cape Town, South Africa). Polyclonal rabbit MKP-1, Raf-1, MEK, and ERK antibodies were from Santa Cruz Biotechnology, Inc. (Santa Cruz, CA). Polyclonal antiactive ERK (threonine and tyrosine phosphorylated, p42 and p44) was from New England Biolabs, Inc. (Beverly, MA). Secondary peroxidase-coupled antirabbit antibodies were from Amersham International. MG132 was from Calbiochem (La Jolla, CA), and U0126 from Promega Corp. (Southampton, UK). All other chemicals, including tissue culture media, *O*-tetradecanoylphorbol 13-acetate (TPA), levamisole, and sodium orthovanadate were of the highest grade, obtained from Sigma (St. Louis, MO).

Cell culture

MBA-15.4 mouse bone marrow stromal cells were a kind gift from Professor S. Wientroub (Tel Aviv University, Israel). They express osteoblastic markers such as alkaline phosphatase and collagen type I but very low levels of PTH receptors *in vitro* and can be induced to produce bone *in vivo* (33). Similarly, the MG-63 human preosteoblast cell line express 1,25-dihydroxyvitamin D3-inducible alkaline phosphatase activity (34) and low levels of PTH receptor (35). MBA 15.4 cells were grown in bicarbonate-buffered DMEM with 10% heat-inactivated fetal calf serum (FCS), 100 U/ml penicillin and 100 μg/ml streptomycin. MG-63 cells were grown in MEM. For experiments, 70% confluent cells were lifted with a rubber policeman and seeded in 24-well plates (proliferation studies), or 100-mm culture dishes (all other experiments). Medium was changed to DMEM with 0.5 or 1% FCS for 24 h to serum-starve and synchronize the cell cycle of the cells before 20% FCS or TPA stimulation. The cell lines did not tolerate serum-free culture but survived 48-h periods in 0.5 or 1% FCS. In experiments involving Dex treatment, cells were cultured to 50% confluence in medium with 10% FCS. Fresh medium containing either 1%, 10%, or 20% FCS was added as indicated for 48 h, along with the substances to be tested.

Cell proliferation

DNA synthesis was assessed by measurement of (^{3}H)-thymidine incorporation into acid-insoluble material, as previously described (36). Briefly, MBA-15.4 or MG-63 cells were grown in 24-well plates in DMEM with 10% FCS. To investigate the effect of Dex, progesterone and RU486 on proliferation, the medium in 50% confluent cultures was replaced with fresh medium containing 10% FCS, to which 10^{-7} M Dex, 10^{-7} M progesterone, and/or 10^{-6} M RU486 were added for 48 h. In every experiment, 2 μCi/ml (^{3}H)-thymidine was added to the medium for the last 2 h of incubation. The incubation was stopped on ice, the medium was removed and the cells were washed twice with ice-cold PBS before being quick-frozen at −70 C. After lysis with 0.1 M NaOH-0.1% sodium dodecyl sulfate at room temperature (21 C), protein and DNA were precipitated with cold trichloroacetic acid at a final concentration of 20% overnight at 4 C, the pellet was washed once with cold 10%

trichloroacetic acid before it was dissolved in 0.1 M NaOH. Aliquots were counted in Ready Gel aqueous scintillation fluid (Beckman Coulter, Inc., Fullerton, CA) to obtain a measure of (^{3}H)-thymidine incorporation.

Western blotting

Cell lysates were prepared by sonication in Tris-buffered saline, containing phosphatase inhibitors (100 μM Na_3VO_4, 50 mM NaF, and 1 mM levamisole) and protease inhibitors (1 mM phenylmethylsulfonylfluoride; 1 μg/ml each of aprotinin, leupeptin, and pepstatin). Protein concentrations were determined using the Bradford method (37), and equal-protein samples (~1 μg/μl) were prepared for electrophoresis according to standard methods. Proteins were separated by SDS-PAGE on 10 or 12% polyacrylamide gels, followed by Western blotting. Western blots of gels were analyzed using antibodies as indicated, followed by enhanced chemiluminescence detection.

pNPP phosphatase assay

Activity was measured at 37 C in a 200 μl incubation mixture (50 mM Tris, 1 mM EDTA, 10 mM dithiothreitol, 1 mM phenylmethylsulfonylfluoride, and 5 mM levamisole) to which 50 μl pNPP (55 mM) was added. The reaction was terminated after 1 h by addition of 800 μl of 0.1 M NaOH, and the absorbance was determined at 410 nm.

Quantitative real-time PCR of CL100 (human MKP-1), 3CH134 (mouse MKP-1) and Pyst (human MKP-3)

Total RNA was extracted from approximately 1×10^6 cells using a High Pure RNA Isolation Kit and treated with deoxyribonuclease 1 (Roche Diagnostic Systems, Mannheim, Germany). The integrity and purity of the RNA was confirmed by agarose gel electrophoresis and absorbance ratios at $A_{260/280}$. Reverse transcription was performed with an oligo(deoxythymidine)$_{12–18}$ primer in 20 μl reaction volume, containing 3–5 μg deoxyribonuclease 1-treated RNA, according to manufacturer's instructions (Life Technologies, Inc., Gaithersburg, MD).

Gene transcript levels of the house keeping gene, glyceraldehyde-3-phosphate dehydrogenase (GAPDH), and the dual-specificity phosphatases CL100, Pyst1 and 3CH124 were quantified by real-time PCR on a LightCycler (Roche Diagnostic Systems). Hot start PCR was performed according to manufacturer's instructions with a final concentration of 3 mM $MgCl_2$ and 0.5 μM primer (LightCycler-FastStart DNA Master SYBR Green I, Roche Diagnostic Systems). The various gene transcript levels of the dual specificity phosphatases in treated samples were quantified and compared with the respective transcript levels in untreated controls using the relative standard curve method (Applied Biosystems, division of Perkin-Elmer, Foster City, CA). Briefly, variation in cDNA concentration in different samples was corrected for using the housekeeping gene—the concentration of GAPDH in each cDNA sample was calculated and the cDNA diluted to contain equal amounts of GAPDH. Standard curves for both human and mouse GAPDH, CL100, 3CH134, and Pyst1 were generated by performing a dilution series of the untreated control cDNA. The relative amount of gene transcript present at different time points were calculated and normalized by dividing the calculated value for the gene of interest by the housekeeping gene value at that particular time point. The amount of gene transcripts at any given time point is expressed relative to the amount of transcript present in the untreated control. A total of three independent experimental repeats were performed, and repeat assessments of cDNA from each experiment were also made.

The following primer pairs were used: human GAPDH (accession no. J04038) forward 5′-AAGGTCGGAGTCAACGGATT-3′, reverse 5′-CTCCTGGAAGATGGTGATGG-3′;

Europe PMC Funders Author Manuscripts

mouse GAPDH (accession NM_008084) forward 5′-ATTGTCAGCAATGCATCCTG-3′, reverse 5′-ATGGACTGTGGTCATGAGCC-3′; human MKP-1, CL100 (accession no. X68277) forward 5′-GTACATCAAGTCCATCTGAC-3′, reverse 5′-GGTTCTTCTAGGAGTAGACA-3′; mouse MKP-1, 3CH134 (accession no. X61940) forward 5′-ACAACAATGACTTGACCGCA-3′, reverse 5′-GGAATGGTTAATACTGGTGG-3′; human MKP-3, PYST1 (accession no. X93920) forward 5′-GCCGCAGGAGCTATACGAGT-3′, reverse 5′-CCGTATTCTCGTTCCAGTCG-3′. As a negative control for PCR contamination, purified mRNA, before RT-PCR, was used as template for PCR reactions with all of the above mentioned primer pairs. No PCR products were detected. To further eliminate possible variation in quantitative PCR due to the presence of residual contaminating DNA, the human and mouse GAPDH primer pairs were designed to span the first and third, and the third and fourth intron/exon boundaries, respectively. Several primer pairs were initially investigated using conventional PCR as genes belonging to the dual-specificity phosphatase family were generally difficult to amplify. Initial attempts using primer pairs designed in the active site region resulted in no target amplification in the absence of PCR additives. The addition of betaine did allow the amplification of target template, but these conditions were unsuitable for real-time PCR as the PCR efficiency was poor and variable. Primers for the MKP-1 gene products, CL100 and 3CH134, used in this study were designed close to the 3′ end of the gene, just after the stop codon and before the poly-A tail initiation codon. These primers amplified target template readily with minimal primer-dimer interference and the high efficiency necessary for accurate quantitative PCR. The identities of all PCR products were confirmed by sequencing.

Statistical analysis

All results obtained are expressed as the mean ± SEM or ± SD as indicated. The significance of differences was calculated either by the Student's one-tailed *t* test, or one-way ANOVA with Dunnet's *post hoc* test. A difference between treatment groups was considered significant at $P < 0.05$.

Results

Dex inhibits osteoblastic proliferation, and this can be prevented by treatment with the GR antagonist, RU486

Dex treatment inhibits osteoblast cell line proliferation (Fig. 1A). When compared with progesterone, only Dex-inhibited cell proliferation significantly ($P < 0.05$). When cells were concurrently treated with Dex and the GR antagonist, RU486, this inhibitory effect was completely blocked, suggesting that the mechanism of growth inhibition is GR dependent. This effect was also found in the human osteoblast MG-63 cell line (Fig. 1C). Because RU486 is an antagonist for both progesterone and GRs (38), the involvement of progesterone in osteoblastic proliferation was tested (Fig. 1A). Progesterone had no effect on MBA-15.4 cell proliferation, either alone or in combination with RU486, suggesting that RU486 primarily acts via the GR in this case. Note that 1 μM Dex produces a more profound impairment of proliferation, but 0.1 μM Dex was used here to accommodate use of a 10-fold excess of RU486. The inhibition of osteoblastic cell proliferation by Dex was partially (Fig. 1B) and completely (Fig. 1D) reversed by the PTP inhibitor, sodium orthovanadate, indicating the involvement of PTPs in this process in both mouse and human osteoblast cell lines (3).

PTPs are the most active cytosolic phosphatases in preosteoblast cell lines

Osteoblastic phosphatase activity was measured by pNPP hydrolysis in the presence of inhibitors for specific phosphatase classes. Sodium orthovanadate inhibited 65–70% of

cytosolic phosphatase activity at pH 7 (Fig. 2A), indicating that PTPs are the dominant active phosphatase class in these immature cells. Sodium fluoride, an inhibitor of serine/threonine phosphatases, weakly inhibited total phosphatase activity, and in combination with vanadate, all activity was abolished (Fig. 2A). Because alkaline phosphatase is a marker of mature osteoblast function, we measured its activity against pNPP using the nonintestinal alkaline phosphatase inhibitor, levamisole. At alkaline pH (pH 9), levamisole inhibited total phosphatase activity by 20% (Fig. 2B), demonstrating the alkaline phosphatase activity present in this osteoblast cell line. At neutral and acidic pH, there was little detectable alkaline phosphatase activity (Fig. 2B), and the assays reported in A and C were carried out at pH 7.5. When cells were treated for 48 h with 10^{-7} M Dex, there was a significant increase in total phosphatase activity (Fig. 2C), indicating up-regulation of these enzymes by the GC.

ERK activity is central to serum-induced osteoblastic proliferation

Treatment of MBA-15.4 cells for 48 h with Dex impairs the activation of ERK in response to mitogens (Fig. 3A, see *arrowheads* at 30 and 60 min). Proliferation in response to fetal calf serum (Fig. 3) and TPA (39) is strongly dependent on MEK-ERK activation. The effect of inhibition of MEK-1 and-2 on ERK activity is illustrated in Fig. 3B. The activation of ERK, following both 5 and 30 min of FCS stimulation, was markedly reduced by pretreatment with the MEK inhibitor, U0126. The effect of this inhibition of ERK on MBA-15.4 cell proliferation is shown in Fig. 2C. It is clear that at all three doses of U0126 used, FCS-induced proliferation was completely blocked. This indicates that MEK and ERK activity is essential for serum-driven preosteoblastic proliferation.

Negative effects of Dex on sustained ERK activation are detectable within 1 h and increase in severity with time

MBA-15.4 mouse (Fig. 4, A and B) and MG-63 human (Fig. 4, A and C) osteoblast cell lines were cultured to subconfluence, serum-starved in 1% FCS for 24 h, pretreated with 1 μM Dex for 5 min to 24 h, before cotreatment with 100 ng/ml TPA for 1 h. Times given indicate total exposure to Dex (one single treatment, pre- and concurrent with TPA). Western blotting for dual-phosphorylated ERK revealed a time-dependent decrease in ERK phosphorylation in both cell lines. This first became apparent following 65 min of treatment, and by 2 h the decrease was consistent. This time point was therefore used in future experiments. The time point of 65 min was initially chosen because we suspected possible rapid, membrane effects of Dex in addition to effects on gene transcription. However, subsequent experiments using Dex treatments of under 30 min did not support this possibility, the only significant repression being produced by ethanol solvent control (results not shown).

Protein synthesis is necessary for normal down-regulation of ERK activity

ERK phosphorylation in response to mitogenic stimulation of osteoblast cell lines peaks by 5 min, thereafter slowly decreasing back to baseline, some time after 4 h of TPA treatment (Fig. 5A; Fig. 5B, *solid line*). However, when *de novo* protein synthesis was inhibited by 2 h pretreatment with 40 μg/ml cycloheximide, peak stimulation of ERK phosphorylation was unaffected, but thereafter was completely stable for more than 4 h (Fig. 5A, *dashed line* in Fig. 5B). Doses of cycloheximide ranging from 1–20 μg/ml all had the same effect on ERK phosphorylation as 40 μg/ml (Fig. 5C). This is in agreement with our previously published results, where ERK activity was assayed for myelin basic protein kinase activity (3) and suggests the action of an inducible nuclear phosphatase.

Dex impairment of ERK phosphorylation is dependent on GR, protein synthesis and PTP activity

A 2-h treatment with Dex (1 h pretreatment, 1 h cotreatment), slightly but significantly ($P < 0.05$) impairs sustained (1 h), mitogen-stimulated ERK phosphorylation (Fig. 5, D and E). This effect is more pronounced with longer exposure to Dex (see Figs. 3A and 4), but the rapid effects of Dex are the focus of the present study, and therefore the 2-h time point was used. Inhibition by Dex was completely reversed by cotreatment with the GR antagonist, RU486, the protein synthesis inhibitor, cycloheximide and the PTP inhibitor, vanadate (Fig. 5, D and E). In fact, as shown in Fig. 5A, cycloheximide potentiates the activation of ERK, even in the absence of Dex. Dex therefore appears to super-stimulate a natural down-regulator of ERK, presumably via a classical GR-dependent, transcriptional mechanism. Neither RU486 (Fig. 5, D and E) nor vanadate (not shown) potentiate the effects of TPA at the doses used. Vanadate, cycloheximide, and RU486 appeared to have a greater effect in the presence of Dex and mitogen than with mitogen alone, but inter-experimental variation was high and the differences are not statistically significant (RU486, $P = 0.11$; cycloheximide, $P = 0.43$).

Dex up-regulates gene expression of the dual-specificity MAPK phosphatase, MKP-1, in both mouse and human osteoblast cell lines

The effect of the GC, Dex, on transcript abundance of human and mouse MKP-1 was investigated using quantitative real-time PCR (See Fig. 6). The relative standard curve method was used and changes in transcript abundance are expressed as fold difference compared with untreated samples (Table 1). GAPDH was used as a GC-insensitive housekeeping gene (Fig. 6A) (40). The data shown in Table 1 are the average of three separate experimental repeats, from cell culture to real-time PCR. The expression of both CL100 (human MKP-1; Fig. 6B) and 3CH134 (mouse MKP-1; Fig. 6C) were found to be approximately 10-fold up-regulated after 30 min of Dex treatment and gene transcript levels stayed elevated for up to 24 h (Fig. 6, B and C). Expression of mouse MKP-1, 3CH134, declines gradually after 1 h of Dex treatment, but still shows an approximate 6-fold increase after 24 h of treatment.

Dex down-regulates expression of MKP-3

The expression pattern of Pyst1 (human MKP-3) was examined using the same experimental cDNA as for human MKP-1, above. In contrast to MKP-1, MKP-3 was only slightly up-regulated after 30 min of Dex treatment and was subsequently strongly down-regulated, with an approximate 10-fold decrease in transcript abundance after 24 h of Dex treatment (Fig. 6D; Table 1). MKP-3 expression following 8 h of treatment was 20-fold down-regulated, but the 8-h time point was only tested twice, and further experiments are necessary to confirm this. The down-regulation of MKP-3 was unexpected because MKP-3 is widely accepted as an ERK-specific MKP (41). However, Kassel *et al.* (26) also found down-regulation of MKP-3 by Dex at the protein level in mast cells.

Dex up-regulates MKP-1 protein levels and concurrently inhibits ERK phosphorylation

MKP-1 levels in cells growing normally in 10% FCS are undetectable by Western blot in both MG-63 (Fig. 7A), and MBA-15.4 cell lines (Fig. 7B). Upon treatment with Dex, MKP-1 levels start to increase, becoming clearly visible within 1 h in MG-63s (Fig. 7A) and appearing after 8 h in MBA-15.4 cells (Fig. 7B). Addition of the 26S proteasome inhibitor, MG132, dramatically enhanced levels of MKP-1 protein. There was a more than 10-fold induction in both cell lines following 4–8 h of Dex treatment (Fig. 7, A and B). Note that a second protein band appears with MG132 treatment in the MBA-15.4 cell line (Fig. 7B). The lower band at M*r* 38 is MKP-1 (42), whereas the M*r* 42 band is likely to be MKP-2 (42)

because the antibody is reported to show some cross-reactivity (Santa Cruz Biotechnology, Inc.). With MG132 pretreatment, MKP-1 levels were also seen to be elevated by Dex after 2 h of treatment in MBA-15.4 osteoblasts, suggesting that the up-regulation of MKP-1 protein has similar dynamics in terms of time and intensity in both cell lines, but that proteasomal degradation is more active in MBA-15.4s. Interestingly, MG132 also increased phosphorylation of ERK in Dex-treated and untreated cells (not shown). This was totally unexpected, and perhaps reflects inhibition by MG132 of lysosomal receptor breakdown, following mono-ubiquitination and receptor endocytosis, as opposed to a 26S proteasome effect (43). Reduced endosomal sorting of growth factor receptors should lead to an increased or more stable pool of active receptors, leading to enhanced down-stream activation of ERK. Because MKP-1 was virtually undetectable in MBA-15.4s in the absence of MG132, we could not use this cell line to study ERK dephosphorylation in the presence of increasing MKP-1 levels.

However, MKP-1 was readily detectable in Dex-treated MG-63 cells in the absence of MG132, and we therefore quantified MKP-1 expression under different mitogenic conditions (Fig. 7C), stripped the blot and reprobed for phosphorylated ERK (Fig. 7D). There was no MKP-1 detectable in serum-starved cells (lane 1, Fig. 7C), but faint bands appeared following 4 h and 7 h Dex treatment (lanes 3 and 4). In lanes 2–4, cells were treated with TPA for 5 min to activate ERK for the phosphorylated ERK (P-ERK) blot in Fig. 7D, and as expected this short treatment had no effect on MKP-1 levels. In lanes 5–7, cells were stimulated for 2 h with the potent mitogenic cocktail, 20% FCS. As described in the literature (25), MKP-1 levels were increased by sustained mitogen stimulation (lane 5, Fig. 7C). Dex pretreatment for 4 h or 7 h substantially enhanced MKP-1 expression on top of the expression induced by serum (lanes 6 and 7; Fig. 7C). This effect was even clearer in cells growing normallly (unstarved) in 10% FCS (lanes 8 and 9), where the baseline levels of MKP-1 expression were lower. When this same blot was stripped and reprobed for P-ERK content (Fig. 7D), both TPA and 20% FCS strongly activated ERK (lanes 2 and 5). Lanes 3 and 4 display low levels of MKP-1 expression and little ERK dephosphorylation, compared with TPA alone, as expected because we have found Dex to have its greatest effects on the sustained phase of ERK activation. Lanes 6 and 7 contained high levels of MKP-1 and showed 20–30% less ERK phosphorylation than lane 5 (20% FCS alone). In lanes 8 and 9 (cells growing normally in 10% serum), there was an 8-fold difference in MKP-1 expression levels induced by Dex treatment, and a 90% decrease in ERK phosphorylation. This result was reproducible, and establishes a clear correlation between increased MKP-1 expression and dephosphorylation of ERK. MKP-1 can also dephosphorylate JNK and p38 (44), but these kinases are expressed at low levels in MBA-15.4 and MG-63 osteoblast cell lines, and we could not detect any phosphorylation under the mitogenic conditions described here. However, treatment with 1 m_M hydrogen peroxide as a positive control strongly activated both JNK and p38 (results not shown).

Discussion

In this study, we report that the inhibitory effects of the GC, Dex, on proliferation of both mouse and human osteoblast cell lines were prevented by the GR antagonist, RU486. Furthermore, we show for the first time that the repression of ERK activation seen following GC treatment is also fully prevented by treatment with RU486, and by the protein synthesis inhibitor, cycloheximide. This provides the first evidence that the negative consequences of GC treatment on osteoblast proliferation may entirely be accounted for by a transcriptional mechanism. The PTP inhibitor, sodium orthovanadate, also prevented the GC-induced decrease in proliferation of both mouse (MBA 15.4) and human (MG-63) immature osteoblast cell lines and reversed the deficit in ERK activation induced by Dex treatment, suggesting that PTPs play an important role in this process. Total phosphatase activity was

increased by Dex treatment, and we now report that the dual-specificity phosphatase, MKP-1, is potently up-regulated at both mRNA and protein levels by Dex. This correlates precisely, in both timing and intensity, with ERK dephosphorylation in the same samples.

Proliferation of osteoblast cell lines in response to fetal calf serum was completely dependent upon MEK and ERK activity, as evidenced by the marked inhibition of both ERK phosphorylation and cell proliferation upon treatment with the MEK inhibitor U0126. Similarly, Dex treatment markedly attenuated ERK response to fetal calf serum, particularly during the sustained phase of ERK activation, which is associated with nuclear translocation and cell cycle activation (20). This sustained phase of ERK activation was both stimulated and prolonged by cycloheximide pretreatment, as described previously using a myelin basic protein kinase activity assay (3), and confirmed here using an antibody specific for dual-phosphorylated ERK (45). Initial ERK activation in the first minutes following mitogen stimulation is unaffected by cycloheximide treatment, the disinhibition only becoming apparent 30 min after mitogen treatment. This is the earliest possible time that MKP-1 protein could start to become available to act on ERK, and the effect of cycloheximide increases steadily following 1, 3, and 4 h of concurrent mitogen stimulation in the presence of the protein synthesis inhibitor. This matches the timing of Dex effects, suggesting a primary effect of the Dex-induced gene product on the sustained phase of ERK activation.

PTPs are generally described as negative regulators of cell proliferation and we found vanadate-sensitive PTPs to be the dominantly active cytosolic phosphatase species in immature, proliferating osteoblast cell lines. Total phosphatase activity was up-regulated by Dex treatment. Specifically, the MAPK inhibitory dual-specificity phosphatase, MKP-1, was 10-fold up-regulated at the mRNA level within 30 min of commencing Dex treatment in both mouse and human osteoblast cell lines. Furthermore, MKP-1 mRNA remained up-regulated for over 24 h following Dex treatment. Protein levels were detectably elevated within 1 h of Dex treatment and increased steadily to a peak between 4 and 8 h. This correlated precisely with dephosphorylation of ERK, suggesting that ERK is a major substrate of this nuclear phosphatase. In direct contrast, the MAPK phosphatase, MKP-3, was slightly up-regulated by Dex after 30 min of treatment and thereafter was markedly down-regulated in the same cDNA samples in which MKP-1 was up-regulated. MKP-3 down-regulation was maximal between 8 and 24 h of Dex treatment, cells containing between 10- and 20-fold less MKP-3 mRNA than untreated cells. This confirms the report by Kassel *et al.* (26), who found down-regulation of MKP-3 by Dex at the protein level in mast cells. MKP-1 is vanadate sensitive (19, 26) and has been reported to mediate Dex-induced inhibition of mast cell proliferation, via rapid GR- and protein synthesis-dependent up-regulation, and consequent dephosphorylation of ERK (26). Therefore MKP-1 up-regulation provides a novel and rapid mechanism, accounting for at least some of the direct inhibitory effects of GCs on both immune and bone cells.

Dex treatment of osteoblast cell lines causes a marked decrease in ERK phosphorylation during the sustained phase (30 min plus) of mitogen-induced ERK activation, commonly regarded as necessary for nuclear shift of ERK and cell cycle activation (11). Up-regulation of MKP-1 mRNA is already clearly detectable following 30 min of Dex treatment, indicating immediate-early gene type regulation, with no prior requirement for transcriptional complex component synthesis (46). Protein synthesis follows, detectable increases in MKP-1 protein levels being seen as early as 1 h following Dex treatment of MG-63 cells and increasing to a peak between 4–8 h in both mouse and human osteoblast lines. Levels remain elevated for at least 24 h following Dex treatment, providing a substantial window of time during which the excess of MKP-1 can prematurely dephosphorylate ERK, with consequent impairment of cell cycle activation. MKP-1 is widely reported to be a high turnover protein, subjected to rapid and controlled degradation

by the 26S proteasome (25). Indeed, we found that use of the proteasomal blocker, MG132, revealed a 10- to 20-fold induction of MKP-1 protein following 6–8 h of Dex treatment in both mouse and human osteoblast lines. The inhibitor only prevents breakdown of protein that has been synthesized and has already had a chance to dephosphorylate substrate proteins such as ERK, so MG132-treated cells give a more accurate and appropriate index of MKP-1 protein levels. Interestingly, human MG-63 cells had higher levels of detectable MKP-1 in the absence of proteasome inhibition than the MBA 15.4 mouse cell line. However, both cell lines showed equivalent up-regulation of MKP-1 mRNA, in both time and quantity, and also very similar protein up-regulation dynamics following MG-132 treatment. Perhaps the difference visible in non-MG132-treated cells illustrates a more rapid proteasomal degradation of MKP-1 in MBA-15.4s than in MG-63s. In fact, MG-63s are more rapidly and consistently affected by Dex than are MBA-15.4s (results not shown), perhaps due to a more persistent pool of active MKP-1.

The dynamics of ERK inhibition by Dex in these osteoblast cell lines are interesting. There are many reports in the literature of rapid, nongenomic effects of GCs on signaling pathways in cells (reviewed in Ref. 5). Although several rapid GC effects are described as being dependent on GC:GR interaction (and therefore RU486 susceptible), they are always independent of GR dimerization and *de novo* mRNA and protein synthesis. In addition, nonclassical GC effects take place in seconds to minutes, as opposed to several hours in the case of classical, transcriptional mechanisms. We find little evidence of Dex effects on ERK activation in under 30 min (results not shown) but start to see inhibition of ERK activity within 1–2 h of Dex treatment. This is very rapid for a transcriptional mechanism, and yet it is fully reversible by treatment with RU486 and cycloheximide, indicating complete dependence on both GC:GR interaction and *de novo* protein synthesis. The effect of Dex on ERK activation becomes more and more apparent with increasing time, peaking between 8 and 24 h, which correlates with maximal up-regulation of MKP-1 protein.

Treatment with sodium orthovanadate largely prevents the decreased proliferation caused by high-dose GC treatment of mouse and human osteoblast cell lines. Normal ERK activity is not only important for cell proliferation, but ERK acts as a critical switch between ostoblastic and adipocytic lineage recruitment from undifferentiated marrow stromal precursors (47, 48). Sodium orthovanadate is a potent inhibitor of all tyrosine phosphatases, including the dual-specificity sub-family, and has been extensively tested as an insulinomimetic in the treatment of type II diabetes. It is proposed to act by inhibition of PTPs such as PTP-1B which down-regulates insulin signaling (49, 50), and is reported to effectively restore insulin sensitivity *in vitro* and *in vivo* (51). There are several possible explanations for the reversal by vanadate of GC-induced growth arrest in osteoblasts. One or several PTPs may be directly up-regulated by Dex, resulting in excessive dephosphorylation of tyrosine phosphorylated substrate molecules in mitogenic signaling pathways. We now provide clear evidence that this does happen in osteoblast cell lines, with a GC-driven induction of MKP-1, and ERK as the promitogenic kinase target. Alternatively, Dex may be down-regulating essential receptors, kinases, adaptors or transcription factors in the mitogenic pathway, resulting in a relative excess of PTPs. Furthermore, vanadate, by preventing inactivation of kinases such as ERK, may have indirect downstream effects that inhibit GC-induced transcriptional regulation. These possibilities need to be investigated further using gene knockout and overexpression mutants, *in vivo* and in primary osteoblast cultures.

We have recently tested the effect of vanadium supplementation in a rat model of GC-induced osteoporosis and find that it is well tolerated, with no detectable side effects, and completely prevented the steroid-induced deficits in bone mineral density, bone formation and bone strength (32). Our results indicate that the central mechanism involved in the

negative regulation of immature osteoblast proliferation by GCs is a transcriptionally generated dysregulation of the ERK axis, involving an imbalance of PTP activity *vs.* kinase response to mitogens. The effective prevention of negative GC effects, *in vivo* and *in vitro*, by the PTP inhibitor sodium orthovanadate suggests new avenues for the management of steroid osteoporosis. The present study strongly indicates that selective inhibitors of MKP-1 should now be developed and tested.

Acknowledgments

Dermot Cox and Roche SA are gratefully acknowledged for excellent LightCycler technical support. Thanks to Elmarie Myburgh for technical advice and training.

This work was supported by grants from the Wellcome Trust (to F.S.H., P.H.), Medical Research Council (F.S.H., P.H.) and the National Research Foundation of South Africa (P.H.), and the Harry Crossley Foundation, University of Stellenbosch (P.H.). Y.E. and H.d.W. are recipients of University of Stellenbosch Post-doctoral Fellowships.

Abbreviations

Dex	Dexamethasone
GAPDH	glyceraldehyde-3-phosphate dehydrogenase
GC	glucocorticoid
GR	GC receptor
GRE	GC response element
JNK	c-*jun* NH_2-terminal kinase
MEK	MAPK/ERK kinase
MKP	MAPK phosphatase
P-ERK	phosphorylated ERK
pNPP	paranitrophenylphosphate
PR	progesterone receptor
PTP	protein tyrosine phosphatase
RPTK	receptor protein tyrosine kinases
SHP	Src homology 2 domain-containing phosphatase
TPA	*O*-tetradecanoylphorbol 13-acetate

References

1. Canalis E. Mechanisms of glucocorticoid action in bone: Implications to glucocorticoid-induced osteoporosis. J Clin Endocrinol Metab. 1996; 81:3441–3447. [PubMed: 8855781]
2. Manolagas SC. Birth and death of bone cells: basic regulatory mechanisms and implications for the pathogenesis and treatment of osteoporosis. Endocr Rev. 2000; 21:115–137. [PubMed: 10782361]
3. Hulley PA, Gordon F, Hough FS. Inhibition of MAPK activity and proliferation of an early osteoblast cell line (MBA 15.4) by dexamethasone: role of protein phosphatases. Endocrinology. 1998; 139:2423–2431. [PubMed: 9564854]
4. Brann DW, Hendry LB, Mahesh VB. Emerging diversities in the mechanism of action of steroid hormones. J Steroid Biochem Mol Biol. 1995; 52:113–133. [PubMed: 7873447]
5. Cato A, Nestl S, Mink S. Rapid actions of steroid receptors in cellular signaling pathways. Science's STKE. 2002http://stke.sciencemag.org/cgi/content/full/sigtrans;2002/138/re9

Europe PMC Funders Author Manuscripts

6. Smith E, Coetzee GA, Frenkel B. Glucocorticoids inhibit cell cycle progression in differentiating osteoblasts via glycogen synthase kinase-3β. J Biol Chem. 2002; 277:18191–18197. [PubMed: 11877389]
7. Seger R, Krebs EG. The MAPK signaling cascade. FASEB J. 1995; 9:726–735. [PubMed: 7601337]
8. Marshall CJ. Specificity of receptor tyrosine kinase signaling: transient versus sustained extracellular signal-regulated kinase activation. Cell. 1995; 80:179–185. [PubMed: 7834738]
9. Kerkhoff E, Rapp UR. Cell cycle targets of Ras/Raf signalling. Oncogene. 1998; 17:1457–1462. [PubMed: 9779991]
10. Lai C-F, Chaudhary L, Fausto A, Halstead LR, Ory DS, Avioli LV, Cheng S-L. Erk is essential for growth, differentiation, integrin expression and cell function in human osteoblastic cells. J Biol Chem. 2001; 276:4443–14450.
11. Lou J, Tu Y, Li S, Manske PR. Involvement of ERK in BMP-2 induced osteoblastic differentiation of mesenchymal progenitor cell line C3H10T1/2. Biochem Biophys Res Commun. 2000; 268:757–762. [PubMed: 10679278]
12. Chaudhary LR, Avioli LV. Activation of extracellular signal-regulated kinases 1 and 2 (ERK1 and ERK2) by FGF-2 and PDGF-BB in normal human osteoblastic and bone marrow stromal cells: differences in mobility and in-gel renaturation of ERK1 in human, rat, and mouse osteoblastic cells. Biochem Biophys Res Commun. 1997; 238:134–139. [PubMed: 9299466]
13. Caverzasio J, Palmer G, Suzuki A, Bonjour JP. Mechanism of the mitogenic effect of fluoride on osteoblast-like cells: evidences for a G protein-dependent tyrosine phosphorylation process. J Bone Miner Res. 1997; 12:1975–1983. [PubMed: 9421230]
14. Waterman H, Yarden Y. Molecular mechanisms underlying endocytosis and sorting of ErbB receptor tyrosine kinases. FEBS Lett. 2001; 490:142–152. [PubMed: 11223029]
15. McDonald PH, Lefkowitz RJ. β-Arrestins: new roles in regulating heptahelical receptors' functions. Cell Signal. 2001; 13:683–689. [PubMed: 11602178]
16. Donovan S, Shannon KM, Bollag G. GTPase activating proteins: critical regulators of intracellular signaling. Biochim Biophys Acta. 2002; 1602:23–45. [PubMed: 11960693]
17. Langlois WJ, Sasaoka T, Saltiel AR, Olefsky JM. Negative feedback regulation and desensitization of insulin- and epidermal growth factor-stimulated p21ras activation. J Biol Chem. 1995; 270:25320–25323. [PubMed: 7592690]
18. Andersen JN, Mortensen OH, Peters GH, Drake PG, Iversen LF, Olsen OH, Jansen PG, Andersen HS, Tonks NK, Moller NP. Structural and evolutionary relationships among protein tyrosine phosphatase domains. Mol Cell Biol. 2001; 21:7117–7136. [PubMed: 11585896]
19. Camps M, Nichols A, Arkinstall S. Dual specificity phosphatases: a gene family for control of MAP kinase function. FASEB J. 2000; 14:6–16. [PubMed: 10627275]
20. Chajry N, Martin PM, Cochet C, Berthois Y. Regulation of p42 mitogen-activated-protein kinase activity by protein phosphatase 2A under conditions of growth inhibition by epidermal growth factor in A431 cells. Eur J Biochem. 1996; 235:97–102. [PubMed: 8631373]
21. Neel BG, Tonks NK. Protein tyrosine phosphatases in signal transduction. Curr Opin Cell Biol. 1997; 9:193–204. [PubMed: 9069265]
22. Slack DN, Seternes OM, Gabrielsen M, Keyse SM. Distinct binding determinants for ERK2/p38α and JNK MAP kinases mediate catalytic activation and substrate selectivity of MAP kinase phosphatase-1. J Biol Chem. 2001; 276:16491–16500. [PubMed: 11278799]
23. Hofken T, Keller N, Fleischer F, Goke B, Wagner AC. Map kinase phosphatases (MKP's) are early responsive genes during induction of cerulein hyperstimulation pancreatitis. Biochem Biophys Res Commun. 2000; 276:680–685. [PubMed: 11027531]
24. Wiessner C. The dual specificity phosphatase PAC-1 is transcriptionally induced in the rat brain following transient forebrain ischemia. Brain Res Mol Brain Res. 1995; 28:353–356. [PubMed: 7723634]
25. Brondello JM, Brunet A, Pouyssegur J, McKenzie FR. The dual specificity mitogen-activated protein kinase phosphatase-1 and -2 are induced by the p42/p44MAPK cascade. J Biol Chem. 1997; 272:1368–1376. [PubMed: 8995446]

26. Kassel O, Sancono A, Kratzschmar J, Kreft B, Stassen M, Cato AC. Glucocorticoids inhibit MAP kinase via increased expression and decreased degradation of MKP-1. EMBO J. 2001; 20:7108–7116. [PubMed: 11742987]
27. Noguchi T, Metz R, Chen L, Mattei MG, Carrasco D, Bravo R. Structure, mapping, and expression of erp, a growth factor-inducible gene encoding a nontransmembrane protein tyrosine phosphatase, and effect of ERP on cell growth. Mol Cell Biol. 1993; 13:5195–5205. [PubMed: 8355678]
28. Johnson RB, Henderson JS. Enhancement by sodium orthovanadate of the formation and mineralization of bone nodules by chick osteoblasts in vitro. Arch Oral Biol. 1997; 42:271–276. [PubMed: 9222445]
29. Canalis E. Effect of sodium vanadate on deoxyribonucleic acid and protein syntheses in cultured rat calvariae. Endocrinology. 1985; 116:855–862. [PubMed: 2578950]
30. Lau KH, Tanimoto H, Baylink DJ. Vanadate stimulates bone cell proliferation and bone collagen synthesis *in vitro*. Endocrinology. 1988; 123:2858–2867. [PubMed: 3058461]
31. Yoon HK, Baylink DJ, Lau KH. Protein tyrosine kinase inhibitors block the stimulatory actions of phosphotyrosine phosphatase inhibitors to increase cell proliferation, alkaline phosphatase activity, and collagen synthesis in normal human bone cells. Am J Nephrol. 2000; 20:153–162. [PubMed: 10773618]
32. Hulley PA, Conradie MM, Langeveldt CR, Hough FS. Glucocorticoid-induced osteoporosis in the rat is prevented by the tyrosine phosphatase inhibitor, sodium orthovanadate. Bone. 2002; 31:220–229. [PubMed: 12110438]
33. Benayahu D, Kletter Y, Zipori D, Wientroub S. Bone marrow-derived stromal cell line expressing osteoblastic phenotype *in vitro* and osteogenic capacity *in vivo*. J Cell Physiol. 1989; 140:1–7. [PubMed: 2544612]
34. Franceschi RT, Romano PR, Park KY. Regulation of type I collagen synthesis by 1,25-dihydroxyvitamin D3 in human osteosarcoma cells. J Biol Chem. 1988; 263:18938–18945. [PubMed: 3264282]
35. Fukayama S, Tashjian AH Jr. Stimulation by parathyroid hormone of 45Ca2+ uptake in osteoblast-like cells: possible involvement of alkaline phosphatase. J Biol Chem. 1989; 264:11879–11886. [PubMed: 2545688]
36. Reid LR, Civitelli R, Avioli LV, Hruska KA. Parathyroid hormone depresses cytosolic pH and DNA synthesis in osteoblast-like cells. Am J Physiol. 1988; 255:E9–E15. [PubMed: 2839040]
37. Bradford MM. A rapid and sensitive method for the quantitation of microgram quantities of protein utilizing the principle of protein-dye binding. Anal Biochem. 1976; 72:248–254. [PubMed: 942051]
38. Bigsby RM, Young PC. Progesterone and dexamethasone inhibition of uterine epithelial cell proliferation: studies with antiprogesterone compounds in the neonatal mouse. J Steroid Biochem Mol Biol. 1993; 46:253–257. [PubMed: 8664174]
39. Langeveldt CR, Engelbrecht Y, Hough FS, Hulley PA. Alternative insulin signalling pathways in osteoblasts. Bone. 2002; 30:7S. (Abstract).
40. Gorzelniak K, Janke J, Engeli S, Sharma AM. Validation of endogenous controls for gene expression studies in human adipocytes and preadipocytes. Horm Metab Res. 2001; 33:625–627. [PubMed: 11607884]
41. Muda M, Theodosiou A, Gillieron C, Smith A, Chabert C, Camps M, Boschert U, Rodrigues N, Davies K, Ashworth A, Arkinstall S. The mitogen-activated protein kinase phosphatase-3 N-terminal noncatalytic region is responsible for tight substrate binding and enzymatic specificity. J Biol Chem. 1998; 273:9323–9329. [PubMed: 9535927]
42. Misra-Press A, Rim CS, Yao H, Roberson MS, Stork PJS. A novel mitogen-activated protein kinase phosphatase. J Biol Chem. 1995; 270:14587–14596. [PubMed: 7782322]
43. Shih SC, Katzmann DJ, Schnell JD, Sutanto M, Emr SD, Hicke L. Epsins and Vps27p/Hrs contain ubiquitin-binding domains that function in receptor endocytosis. Nat Cell Biol. 2002; 4:389–393. [PubMed: 11988742]
44. Slack DN, Seternes OM, Gabrielsen M, Keyse SM. Distinct binding determinants for ERK2/p38α and JNK MAP kinases mediate catalytic activation and substrate selectivity of map kinase phosphatase-1. J Biol Chem. 2001; 276:16491–16500. [PubMed: 11278799]

45. Fincham VJ, James M, Frame MC, Winder SJ. Active ERK/MAP kinase is targeted to newly forming cell-matrix adhesions by integrin engagement and v-Src. EMBO J. 2000; 12:2911–2923. [PubMed: 10856236]
46. Kwak SP, Dixon JE. Multiple dual specificity protein tyrosine phosphatases are expressed and regulated differentially in liver cell lines. J Biol Chem. 1995; 270:1156–1160. [PubMed: 7836374]
47. Jaiswal RK, Jaiswal N, Bruder SP, Mbalaviele G, Marshak DR, Pittenger MF. Adult mesenchymal stem cell differentiation to the osteogenic or adipogenic lineage is regulated by mitogen-activated protein kinase. J Biol Chem. 2000; 275:9645–9652. [PubMed: 10734116]
48. Hu E, Kim JB, Sarraf P, Spiegelman BM. Inhibition of adipogenesis through MAP kinase-mediated phosphorylation of PPAR-γ. Science. 1996; 274:2100–2103. [PubMed: 8953045]
49. Elchebly EM, Payette P, Michaliszyn E, Cromlish W, Collins S, Loy AL, Normandin D, Cheng A, Himms-Hagen J, Chan CC, Ramachanran C, Gresser MJ, Tremblay ML, Kennedy BP. Increased insulin sensitivity and obesity resistance in mice lacking the protein tyrosine phosphatase-1B gene. Science. 1999; 283:1544–1548. [PubMed: 10066179]
50. Chen H, Cong LN, Li Y, Yao ZJ, Wu L, Zhang ZY, Burke TR, Quon MJ. A phosphotyrosyl mimetic peptide reverses impairment of insulin-stimulated translocation of GLUT4 caused by overexpression of PTP1B in rat adipose cells. Biochemistry. 1999; 38:384–389. [PubMed: 9890920]
51. Cohen N, Halberstam M, Shlimovich P, Chang CJ, Shamoon H, Rossetti L. Oral vanadyl sulfate improves hepatic and peripheral insulin sensitivity in patients with non-insulin-dependent diabetes mellitus. J Clin Invest. 1995; 95:2501–2509. [PubMed: 7769096]

Europe PMC Funders Author Manuscripts

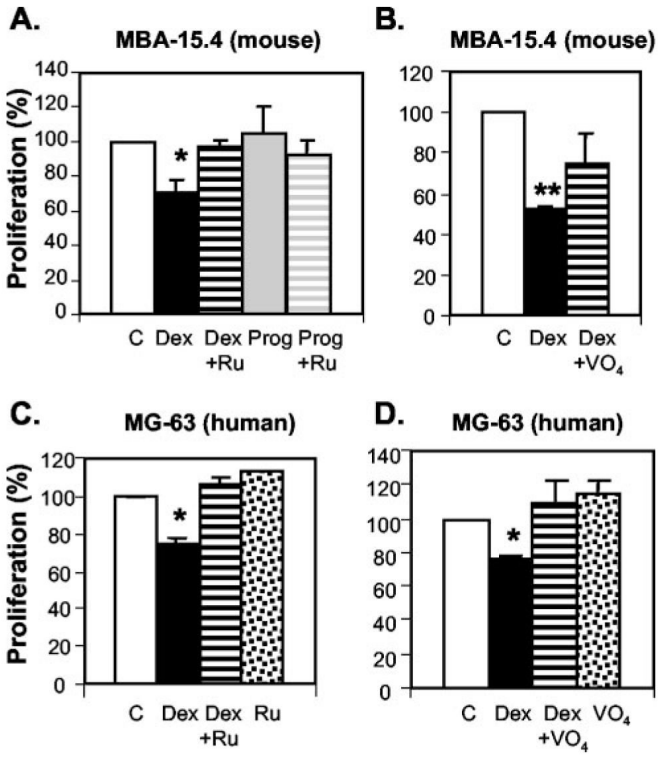

Fig. 1.

Effect of Dex on MBA-15.4 (A, B) and MG-63 (C, D) preosteoblastic cell proliferation. Cells were grown in 10% FCS for 48 h, after which they were stimulated with fresh 10% FCS immediately before treatment with either Dex (10^{-7} M) or Prog (10^{-7} M); with or without concurrent treatment with either 10^{-6} M RU486 or 10^{-6} M Na_3VO_4 for 48 h. Two hours before the reaction was terminated, 2 μCi/ml (^{3}H)-thymidine was added to the medium, and DNA synthesis quantified. Dimethylsulfoxide (0.1%), RU486 (10^{-6} M in 0.1% dimethylsulfoxide), and VO_4 (10^{-6} M) alone were also included as controls. Mean values from three independent experiments (A, C, D) are displayed, mean ± SEM. B, A representative experiment of three identical repeats is shown, mean ± SD. *, $P < 0.05$; **, $P < 0.01$ indicates significant difference to control (Ru, Ru486; Prog, progesterone; VO_4, sodium orthovanadate). *Open bars*, Controls; *black bars*, Dex; *gray bar*, progesterone; *hatched bars*, addition of inhibitor as indicated; *stippled bars*, inhibitors alone.

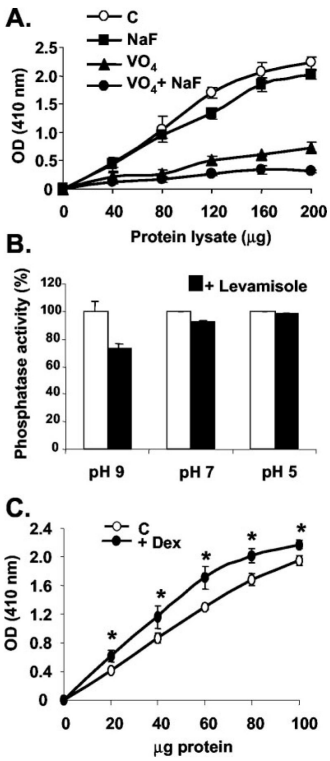

Fig. 2.

Phosphatase activity assays (pNPP-hydrolysis) in MBA-15.4 preosteoblast cell line. Cells were grown until confluent, lysed, and treated in assay with or without 10 mM Na_3VO_4 and/or 50 mM NaF at pH 7.5 (A) or 5 mM levamisole, pH as indicated (B). In addition, cells were grown until 50% confluent, and treated with fresh 10% FCS with or without 10^{-7} M Dex for 48 h (C). The data shown are the means of three repeat experiments, where *, $P < 0.05$; **, $P < 0.001$ (C), or are representative of at least three identical repeats (A, B).

Europe PMC Funders Author Manuscripts

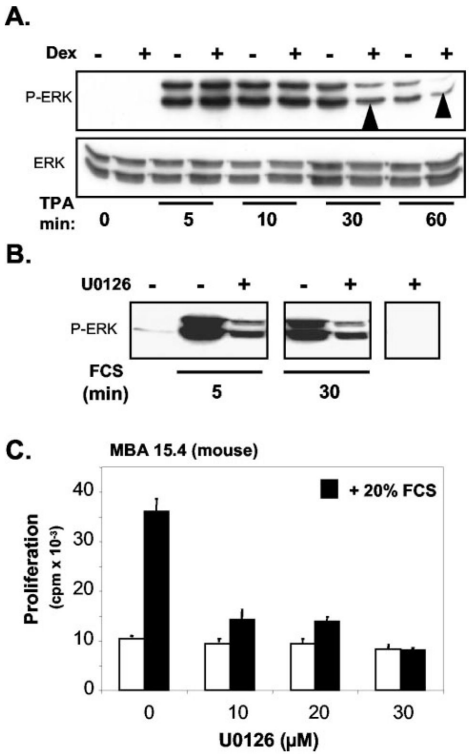

Fig. 3.

Effect of Dex on TPA-stimulated ERK activity in MBA-15.4 pre-osteoblast cell line (A). Subconfluent MBA-15.4 cells were serum-starved overnight in 1% FCS. The cells were subsequently treated with or without 10^{-7} M Dex for 48 h and then treated with 100 ng/ml TPA as indicated. Cells were lysed and ERK activity was visualized by Western blot analysis using an antibody specific for dual-phosphorylated ERK. Detection of total is ERK is indicated below. B, Effect of inhibition of MEK-1 and -2 on ERK activity in MBA 15.4 preosteoblastic cells. Subconfluent MBA-15.4 cells were serum-starved overnight in 1% FCS, incubated (30 min) with or without 10 μM U0126 and then treated with 20% FCS for 5 or 30 min. Dual-phosphorylated ERK in equal protein samples was detected as described above. C, The effect of different doses of U0126 on MBA 15.4 preosteoblast cell proliferation. Fifty percent confluent cells were serum-starved overnight in medium containing 0.5% FCS. The cells were then pretreated for 30 min with increasing concentrations of U0126, followed by addition of 20% FCS for a further 24 h. DNA synthesis was measured as described in Fig. 1. Results are shown as mean ± SD of three identical experiments.

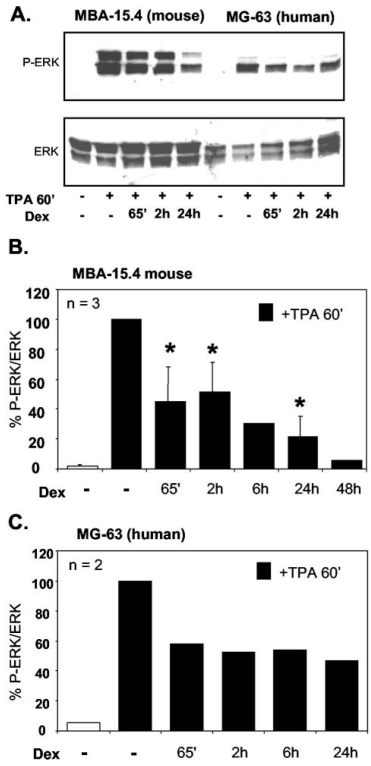

Fig. 4.

Dexamethasone inhibits ERK phosphorylation within 1 h and the effect is sustained. MBA-15.4 (A, B) and MG-63 (A, C) cells were grown to subconfluence, serum starved in 1% FCS for 24 h, and pretreated with 1 μ_M Dex for 5 min to 24 h as indicated. 100 ng/ml TPA was added to the cultures for 1 h following Dex treatment. Times indicate total exposure to Dex. (A) is a representative Western blot showing total ERK and dual-phosphorylated ERK (B) and (C) are the average of three and two independent experiments, respectively, where blots were stripped and reprobed to quantitate and correct for total ERK levels; ERK phosphorylation is expressed as a percentage of maximum stimulation with TPA alone. *, $P < 0.05$ *vs.* TPA alone.

Europe PMC Funders Author Manuscripts

Europe PMC Funders Author Manuscripts

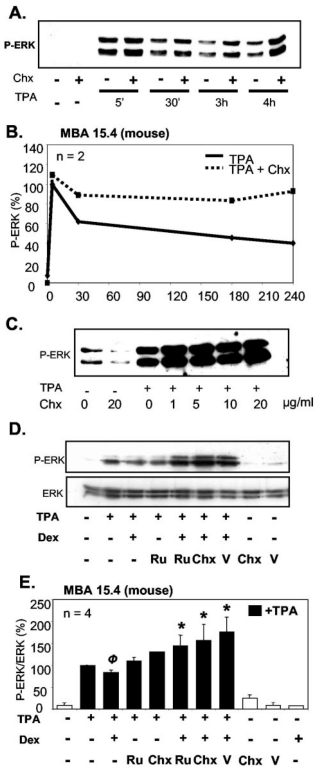

Fig. 5.

Inhibition of ERK phosphorylation is dependent on protein synthesis, GC:GR interaction, and PTP activity. MBA-15.4 cells were serum starved in 1% FCS for 24 h, treated for 2 h with 40 μg/ml cycloheximide (A, B), or 1–20 μg/ml cycloheximide as indicated (C) and then stimulated with 100 ng/ml TPA for 5 min to 4 h as indicated (A, B) or 4 h (C). Phosphorylation of ERK was quantified in samples normalized for total ERK content. C and D, MBA-15.4 osteoblasts were serum starved in 1% serum overnight, pretreated for 1 h with 1 μ_M Dex alone or in combination with either 1 μ_M RU486, 40 μg/ml cycloheximide or 1 μ_M sodium orthovanadate, and then stimulated with 100 ng/ml TPA added for 1 h further. ERK phosphorylation was quantified as above. Total exposure to Dex, RU, cycloheximide, and vanadate was 2 h. A, C, and D, Representative Western blots; B, the average of two experimental repeats; E, the average of four experimental repeats. *, $P<0.05$ *vs.* TPA+Dex; $\Phi = P<0.05$ *vs.* TPA alone.

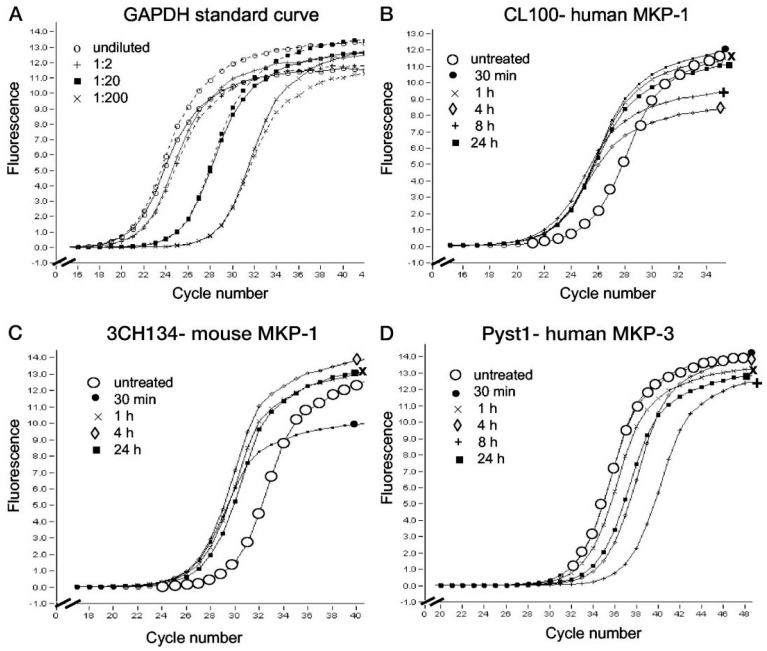

Fig. 6.

MKP-1 mRNA is rapidly up-regulated by Dex, whereas MKP-3 is down-regulated. Real-time PCR was used to quantify expression of the dual-specificity phosphatases 3CH134 (mouse MKP-1), CL100 (human MKP-1), and Pyst1 (human MKP-3) in osteoblast cell lines in response to glucocorticoid treatment. A, Example of a standard curve, GAPDH. B, CL100, approximately 10-fold up-regulation following 30 min of Dex treatment. C, 3CH134, approximately 10-fold up-regulation following 30 min of Dex treatment. D, Pyst1, little initial up-regulation and approximately 10-fold down-regulation following 24 h of Dex treatment. Untreated controls (*large open circles*), treatment with Dex for 30 min (*filled circles*), 1 h (*cross*), 4 h (*diamond*), 8 h (*plus*), 24 h (*filled square*). Template concentration was normalized using the housekeeping gene, GAPDH, and fold differences were calculated using the relative standard curve method (see *Materials and Methods*). Data shown are representative of three independent experiments, and of several duplicate repeats performed on the same batch of cDNA from each experiment (see Table 1).

Europe PMC Funders Author Manuscripts

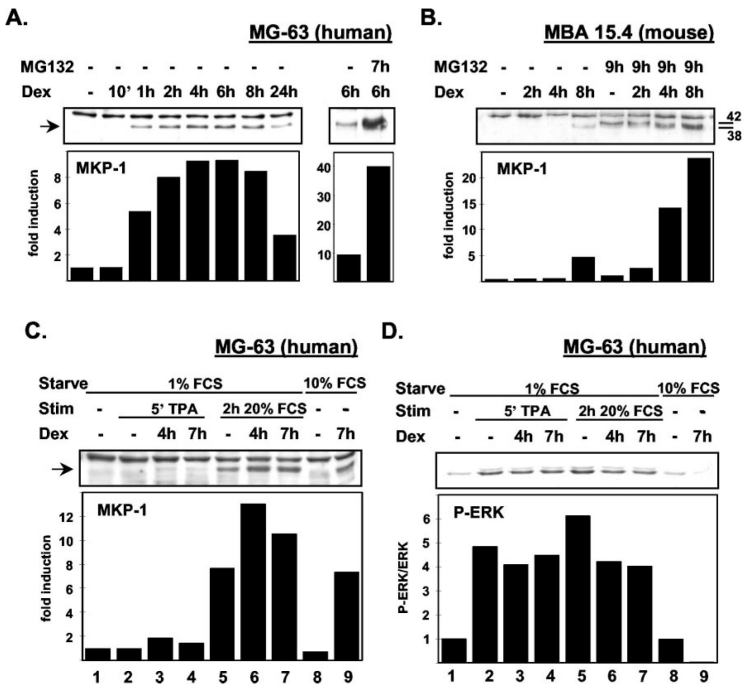

Fig. 7.

MKP-1 protein is markedly up-regulated by Dex treatment and this correlates precisely with dephosphorylation of ERK. Human MG-63 (A) and mouse MBA-15.4 (B) osteoblast cell lines were subjected to 1 μ_M Dex treatment for 1–8 h while growing rapidly in 10% FCS. Because MKP-1 is rapidly degraded following synthesis and action, cells were pretreated for 1 h with the 26S proteasome inhibitor, MG132 (30 μ_M) where indicated. MKP-1 protein was quantified by Western blot and densitometry. MKP-1 up-regulation in human MG-63 cells (C) and concomitant ERK dephosphorylation (D) by 1 μ_M Dex treatment for 4 or 7 h was compared following treatment for 5 min with 100 ng/ml TPA and 2 h with 20% FCS, and also in normally growing MG-63 osteoblasts in 10% serum. Results shown are representative of at least two experimental repeats. P-ERK quantifications in (D) were performed by stripping and reprobing the same blot with antiactive ERK antibody, and densitometric values are normalized for total ERK content.

Europe PMC Funders Author Manuscripts

Europe PMC Funders Author Manuscripts

TABLE 1

Dex-regulated gene expression of the human and mouse dual-specificity MAPK phosphatase MKP-1 and the human dual-specificity MAPK MKP-3 in osteoblastic cell lines

Time post Dex treatment (h)	Relative amount of gene transcript		
	CL100	*3CH134*	*Pyst1*
0	1	1	1
0.5	10.6 ± 3.9[a]	11.0 ± 4.8[a]	1.16 ± 0.5
1	7.3 ± 2.8	11.4 ± 5.1[a]	0.8 ± 0.4
4	9.3 ± 1.8[b]	8.6 ± 3.6[a]	0.4 ± 0.1[b]
8	8.5	7.2	0.08
24	9.9 ± 2.7[b]	6.8 ± 3.1[b]	0.19 ± 0.07[a]

Real-time PCR was used to quantify expression of the dual-specificity phosphatases 3CH134 (mouse MKP-1), CL100 (human MKP-1), and Pyst1 (human MKP-3) in response to glucocorticoid treatment. Data shown are the average of three or four experimental repeats from cell culture to real-time quantitative PCR and are expressed as the mean ± SD, except for the 8-h time point where the average of two repeats is shown. Data were analyzed by one-way ANOVA using Dunnett's *post hoc* test for multigroup comparisons.

[a] $P<0.01$

[b] $P<0.05$